Reinhardt Annekathrin (Orcid ID: 0000-0002-0295-0312)

Sahm Felix (Orcid ID: 0000-0001-5441-1962)

Wefers Annika K (Orcid ID: 0000-0001-9394-8519)

Becker Albert (Orcid ID: 0000-0003-2661-3705)

Schittenhelm Jens (Orcid ID: 0000-0002-9168-6209)

Niehusmann Pitt (Orcid ID: 0000-0002-3247-5241)

Anaplastic ganglioglioma – a diagnosis comprising several distinct tumour types

Annekathrin Reinhardt[1,2*], Kristin Pfister[1,2,32], Daniel Schrimpf[1,2], Damian Stichel[1,2], Felix Sahm[1,2], David E. Reuss[1,2], David Capper[4,5], Annika K. Wefers[1,2,33], Azadeh Ebrahimi[1,2,9], Martin Sill[3,6], Joerg Felsberg[7], Guido Reifenberger[7,8], Albert Becker[9], Marco Prinz[10,11,34], Ori Staszewski[10], Christian Hartmann[12], Jens Schittenhelm[13], Dorothee Gramatzki[14], Michael Weller[14], Adriana Olar[15] , Elisabeth Jane Rushing[16], Markus Bergmann[17], Michael A. Farrell[18], Ingmar Blümcke[19], Roland Coras[19], Jan Beckervordersandforth[20], Se Hoon Kim[21], Fabio Rogerio[22], Petia S. Dimova[23], Pitt Niehusmann[24], Andreas Unterberg[25], Michael Platten[26,27], Stefan M. Pfister[3,6,28,29], Wolfgang Wick[3,30], Christel Herold-Mende[31], Andreas von Deimling[1,2,3]

1 Department of Neuropathology, University Hospital Heidelberg, Heidelberg, Germany

2 Clinical Cooperation Unit Neuropathology, German Cancer Research Center (DKFZ), Heidelberg, Germany

3 German Cancer Consortium (DKTK), Core Center Heidelberg, Germany

4 Charité – Universitätsmedizin Berlin, corporate member of Freie Universität Berlin, Humboldt-Universität zu Berlin, Department of Neuropathology, Berlin, Germany

5 German Cancer Consortium (DKTK), Partner Site Berlin, German Cancer Research Center (DKFZ), Heidelberg, Germany

This article has been accepted for publication and undergone full peer review but has not been through the copyediting, typesetting, pagination and proofreading process which may lead to differences between this version and the Version of Record. Please cite this article as doi: 10.1111/nan.12847

6 Hopp Children's Cancer Center Heidelberg (KiTZ), Heidelberg, Germany

7 Institute of Neuropathology, Heinrich Heine University, Medical Faculty, University Hospital Düsseldorf, Düsseldorf, Germany

8 German Cancer Consortium (DKTK), Partner Site Essen/Düsseldorf, German Cancer Research Center (DKFZ), Heidelberg, Germany

9 Department of Neuropathology, University of Bonn, Bonn, Germany

10 Institute of Neuropathology, Medical Faculty, University of Freiburg, Freiburg, Germany

11 Center for Basics in NeuroModulation (NeuroModulBasics), Faculty of Medicine, University of Freiburg, Freiburg, Germany

12 Department of Neuropathology, Hannover Medical School, Hannover, Germany

13 Institute of Pathology and Neuropathology, University Tübingen, Comprehensive Cancer Center Tübingen, Tübingen, Germany

14 Department of Neurology, University Hospital and University Zurich, Zurich, Switzerland

15 NOMIX Laboratories, Denver, CO, USA

16 Institute of Neuropathology, University Hospital Zurich (USZ), Zurich, Switzerland

17 Institute of Neuropathology, Center for Pathology, Klinikum Bremen Mitte, Bremen, Germany

18 Department of Neuropathology, Beaumont Hospital, Dublin, Ireland

19 Department of Neuropathology, University Hospital Erlangen, Erlangen, Germany, Member of EpiCARE ERN

20 Department of Pathology, GROW School for Oncology and Developmental Biology, Maastricht University Medical Centre, Maastricht, The Netherlands

21 Department of Pathology, Yonsei University, College of Medicine, Seoul, South Korea

22 Department of Pathology, University of Campinas (UNICAMP), Campinas, São Paulo, Brazil

23 Epilepsy Surgery Center, Department of Neurosurgery, St. Ivan Rilski University Hospital, Sofia, Bulgaria

24 Section of Neuropathology, Department of Pathology, Oslo University Hospital, Oslo, Norway

25 Clinic for Neurosurgery, University Hospital Heidelberg, Heidelberg, Germany

26 Department of Neurology, Medical Faculty Mannheim, Heidelberg University, Mannheim, Germany

27 Clinical Cooperation Unit Neuroimmunology and Brain Tumour Immunology, German Cancer Research Center (DKFZ), Heidelberg

28 Division of Paediatric Neurooncology, German Cancer Research Center (DKFZ), Heidelberg, Germany

29 Department of Paediatric Oncology and Hematology, University Hospital Heidelberg, Heidelberg, Germany

30 Neurology Clinic, University Hospital Heidelberg, Heidelberg, Germany

31 Division of Experimental Neurosurgery, Department of Neurosurgery, University Hospital Heidelberg, Heidelberg, Germany

32 Institute of Pathology, Kantonsspital Winterthur, Winterthur, Switzerland

33 Institute of Neuropathology, University Medical Center Hamburg-Eppendorf, Hamburg, Germany

34 Signalling Research Centres BIOSS and CIBSS, University of Freiburg, Freiburg, Germany

* Current address: Centre for Human Genetics Tübingen, Tübingen, Germany

Correspondence:

Prof. Dr Andreas von Deimling

Abteilung Neuropathologie

Im Neuenheimer Feld 224, 69120 Heidelberg

Tel. +49 6221 564651 / Fax +49 6221564566

E-mail: andreas.vondeimling@med.uni-heidelberg.de

Key words:	anaplastic ganglioglioma, ganglioglioma, DNA methylation analysis, methylation class, molecular glioma entities, molecular neuropathology
Running title:	Molecular profiles of anaplastic ganglioglioma
Number of words:	5576
Number of figures:	6
Number of tables:	1

Key points

- Molecular analyses and re-assessment of histological features of tumours designated as anaplastic ganglioglioma revealed a wide spectrum of different entities.
- The majority of study cases could be assigned to established CNS WHO tumour types, whereas the non-assignable tumours were heterogeneous and did not constitute a distinct entity.
- Comprehensive molecular testing of cases with the histological designation of anaplastic ganglioglioma is recommended.

Abstract

Anaplastic ganglioglioma is a rare tumour and diagnosis has been based on histological criteria. The 5th edition of the World Health Organization Classification of Tumours of the Central Nervous System (CNS WHO) does not list anaplastic ganglioglioma as a distinct diagnosis due to lack of molecular data in previous publications. **Aim:** We retrospectively compiled a cohort of 54 histologically diagnosed anaplastic gangliogliomas to explore whether the molecular profiles of these tumours represent a separate type or resolve into other entities. **Methods:** Samples were subjected to histological review, DNA methylation profiling and next generation sequencing. Morphologic and molecular data were summarised to an integrated diagnosis. **Results:** The majority of histologically diagnosed anaplastic gangliogliomas resolved into CNS WHO diagnoses of glial tumours, most commonly pleomorphic xanthoastrocytoma (16/54), glioblastoma, IDH wildtype and diffuse paediatric-type high-grade glioma, H3 wildtype and IDH wildtype (11 and 2/54) followed by low-grade glial or glioneuronal tumours including pilocytic astrocytoma, dysembryoplastic neuroepithelial tumour and diffuse leptomeningeal glioneuronal tumour (5/54), IDH mutant astrocytoma (4/54) and others (6/54). A subset of tumours (10/54) was not assignable to a CNS WHO diagnosis and common molecular profiles pointing to a separate entity were not evident. **Conclusion:** In summary, we show that tumours histologically diagnosed as anaplastic ganglioglioma comprise a wide spectrum of CNS WHO tumour types with different prognostic and therapeutic implications. We therefore suggest assigning this designation with caution and recommend comprehensive molecular workup.

Abbreviations

7/10 signature	combination of gain of chromosome 7 and loss of chromosome 10
aGG	anaplastic ganglioglioma
ALK	Anaplastic Lymphoma Receptor Tyrosine Kinase
ATRX	Alpha Thalassemia/Mental Retardation Syndrome X-Linked
BRAF	v-Raf murine sarcoma viral oncogene homolog B
CC1	Cell Conditioning Solution, Antigen Retrieval Buffer (Ventana Medical Systems, Tucson, Arizona, USA)
CCND2	Cyclin D2
CD	cluster of differentiation
CDK4	Cyclin Dependent Kinase 4
CDKN2A/B	Cyclin Dependent Kinase Inhibitor 2A/B
CNS	central nervous system
CNS WHO	World Health Organization Classification of Tumours of the Central Nervous System
DKFZ	Deutsches Krebsforschungszentrum (German Cancer Research Center)
DNA	desoxyribonucleic acid
EGFR	Epidermal Growth Factor Receptor
ERK	Extracellular Signal-Regulated Kinase 2
EWSR1	Ewing Sarcoma Breakpoint Region 1
EZHIP	EZH Inhibitory Protein
FFPE	formalin-fixed, paraffin-embedded
GBM	glioblastoma
GFAP	glial fibrillary acidic protein
GG	ganglioglioma
H3	H3 histone family protein
H3 K27M	K27M mutation in a Histone H3 family protein
H3 K27me3	immunohistochemical stain indicating tri-methylation of lysine 27 in a Histone H3 family protein
H3-3A	*H3* Histone Gene Family Member 3A
HE	haematoxylin and eosin
HIST1H3B	Histone Cluster 1 H3 Family Member B (*H3C2*)
IDH	isocitrate dehydrogenase protein
IDH1/2	isocitrate dehydrogenase genes 1 and 2
INI1	Integrase Interactor 1
Ki67/MIB-1	marker of proliferation
KRAS	Kirsten Rat Sarcoma Viral Oncogene Homolog
MC	methylation class
MCF	methylation class family
MDM2	Mouse double minute 2 homolog
MET	Hepatocyte Growth Factor Receptor
MYCN	V-Myc Avian Myelocytomatosis Viral Oncogene Neuroblastoma Derived Homolog
NOS	not otherwise specified
PA	pilocytic astrocytoma
PDGFRA	Platelet Derived Growth Factor Receptor Alpha
PIK3CA	Phosphatidylinositol-4,5-Bisphosphate 3-Kinase Catalytic Subunit Alpha
PLAG1	Pleomorphic Adenoma Gene 1
PLAGL1	*PLAG1* Like Zinc Finger 1

PPP1CB	Protein Phosphatase 1, Catalytic Subunit, Beta Isoform
R	programming language
RELA	*NF-Kappa-B* Transcription Factor P65
RNA	ribonucleic acid
RTK	receptor tyrosine kinase protein
SETD2	SET Domain Containing 2, Histone Lysine Methyltransferase
SMARCB1	*SWI/SNF* Related, Matrix Associated, Actin Dependent Regulator Of Chromatin, Subfamily B, Member 1
TERT	Telomerase Reverse Transcriptase
t-SNE	t-distributed stochastic neighbour embedding (in the present context unsupervised comparison of the methylation profiles of aGGs with the methylation profiles of reference classes)
UMAP	Uniform Manifold Approximation and Projection (in the present context unsupervised comparison of the methylation profiles of aGGs with the methylation profiles of reference classes)
V11b4, V12.3, V12.5	versions of the brain tumour classifier; see also: https://www.molecularneuropathology.org/mnp/classifiers
WHO	World Health Organization
ZFTA	Zinc Finger Translocation Associated

Methylation cluster (t-SNE/UMAP)

A IDH	IDH glioma, subclass astrocytoma
A IDH HG	IDH glioma, subclass high-grade astrocytoma
ATRT MYC	atypical teratoid/rhabdoid tumour, subclass *MYC*
DIG/DIA	desmoplastic infantile astrocytoma/ganglioglioma
DLGNT	diffuse leptomeningeal glioneuronal tumour
DMG K27	diffuse midline glioma, H3 K27 altered
DMT SMARCB1	desmoplastic myxoid tumour, *SMARCB1*-mutant
DNET	dysembryoplastic neuroepithelial tumour
EPN RELA	ependymoma, *RELA* fusion-positive
EPN ST 1	neuroepithelial tumour, *PLAGL1* fusion-positive
GBM MES	glioblastoma, mesenchymal subtype
GBM MID	glioblastoma of the midline
GBM MYCN	glioblastoma, *MYCN* subtype
GBM RTK I	glioblastoma, RTK I subtype
GBM RTK II	glioblastoma, RTK II subtype
GBM RTK III	glioblastoma, RTK III subtype
GG	ganglioglioma
HEMI CORT	control tissue, hemispheric cortex
HGAP	high-grade astrocytoma with piloid features
IHG	infantile hemispheric glioma
PA CORT/GG	pilocytic astrocytoma of the supratentorial hemispheres and ganglioglioma
PA MID	pilocytic astrocytoma of the midline
PA PF	pilocytic astrocytoma of the posterior fossa
PXA	pleomorphic xanthoastrocytoma
SEGA	subependymal giant cell astrocytoma
SEPN SUP	supratentorial subependymoma

Methylation classes (brain tumour classifier)

MC (a)PXA	methylation class (anaplastic) pleomorphic xanthoastrocytoma
MC CTRL RB	methylation class control tissue, reactive brain (V11b4)
MC DLGNT (2)	methylation class diffuse leptomeningeal glioneuronal tumour (subclass 2)
MC DMG K27	methylation class diffuse midline glioma, H3 K27 altered
MC DNET	methylation class dysembryoplastic neuroepithelial tumour
MC EPN RELA	methylation class ependymoma, *RELA* fusion-positive (V11b4)
MC EPN RELA like	methylation class ependymoma, *RELA* like (V12.3)
MC EPN ST 1	methylation class neuroepithelial tumour, *PLAGL1* fusion-positive (V12.5)
MC EPN ZFTA	methylation class ependymoma, *ZFTA* fusion-positive (V12.5)
MC GG	methylation class ganglioglioma
MC GLIOMA NORM HI	methylation class glioma with high proportion of normal (immune or stromal) cells (V12.3, V12.5)
MC PA CORT/GG	methylation class pilocytic astrocytoma of the supratentorial hemispheres and ganglioglioma
MCF ATRT	methylation class atypical teratoid/rhabdoid tumour
MCF GBM IDH wt	methylation class family glioblastoma IDH wildtype
MCF HGG H3 wt IDH wt	methylation class family diffuse paediatric-type high-grade glioma, H3 wildtype and IDH wildtype
MCF IDH glioma	methylation class family IDH mutant glioma
MCF LGGNT	methylation class family low-grade glioneuronal tumour
MCF PA	methylation class family pilocytic astrocytoma

Integrated diagnoses

A IDH	astrocytoma IDH mutant, CNS WHO grades 2-4
ATRT	atypical teratoid/rhabdoid tumour, CNS WHO grade 4
DLGNT	diffuse leptomeningeal glioneuronal tumour
DMG K27	diffuse midline glioma H3 K27 altered, CNS WHO grade 4
DNET	dysembryoplastic neuroepithelial tumour, CNS WHO grade 1
GBM IDH wildtype	glioblastoma IDH wildtype, CNS WHO grade 4
IHG	infant-type hemispheric glioma
PA	pilocytic astrocytoma, CNS WHO grade 1
PXA	pleomorphic xanthoastrocytoma, CNS WHO grades 2-3

Introduction

Patients diagnosed with ganglioglioma WHO grade 1 (GG) usually have a favourable clinical outcome with a recurrence rate of 1% and a 10-year overall survival rate of 84-86% [1-3]. Histological features of anaplasia have been observed in about 1-8% of GGs prompting the designation of anaplastic ganglioglioma (aGG) [1, 4-6]. The 5th edition of the World Health Organization Classification of Tumours of the Central Nervous System (CNS WHO) states that anaplasia has been observed in the glial component including conspicuous mitotic activity, high Ki67 proliferation index, necrosis and microvascular proliferation [7]. Based on the data available, patients with aGG fare worse than patients with GG CNS WHO grade 1. Recurrence was observed in 50% of the aGG patients and median overall survival ranged from 25-44 months [2, 5, 6, 8-12]. Similar to GGs, *BRAF* V600E mutations also have been described in aGGs. Other alterations observed in individual cases of aGGs include *CDKN2A*/p16 loss, *CDK4* gain/amplification, p53 accumulation, *TERT* promoter mutations, *ATRX* loss and *H3-3A* K27M mutations [6, 13-17]. However, no characteristic molecular profile has been established so far and the histological features described for this entity allow for an ample range of interpretation. According to the 5th edition of the CNS WHO classification further studies are required to confirm aGG as a distinct tumour type [7]. In the present study we systematically analysed the histological findings and molecular profiles of a cohort of 54 tumours originally diagnosed by histology as aGG in order to explore whether these tumours constitute a distinct group.

Materials and Methods

Tissue samples and clinical data

Tissue samples from 54 patients histologically diagnosed as aGG between the years 2000 and 2018 were collected for this study. Cases were included based on the original diagnosis of the supplier. Formalin-fixed, paraffin-embedded (FFPE) tissue samples of these tumours were retrieved from the archives of the Institutes of Neuropathology in Heidelberg, Erlangen, Bonn, Düsseldorf, Freiburg, Hannover, Tübingen, Bremen Mitte, Zurich, Basel, the Beaumont Hospital Dublin and the University of Texas, MD Anderson Cancer Center. The following clinical data were acquired when possible: histological diagnosis, patient sex, age at diagnosis of aGG, tumour localization and resection state (primary surgery or re-resection).

Histological examination and immunohistochemistry

In order to identify potential associations between histological and molecular profiles haematoxylin and eosin (HE)-stained slides were systematically reviewed by AR and KP with the following histological criteria evaluated for each tumour: general morphological growth pattern, infiltration pattern, cellularity, nuclear pleomorphism, presence of xanthomatous, multinucleated or giant cells, mitoses, necrosis, vascular changes, presence of eosinophilic granular bodies or Rosenthal fibres, lymphocytic infiltration, calcification and the presence of reticulin fibres in the tumour. Reticulin stains were performed in 31 of 54 cases. For tumours with sufficient tissue available, immunohistochemistry with antibodies specific for glial fibrillary acidic protein (GFAP, n=43), synaptophysin (n=44), CD34 (n=32), Ki67/MIB-1 (n=42), ATRX (n=15), H3 K27M (n=2), IDH1 R132H (n=18) or BRAF V600E (n=36) was performed on a Ventana BenchMark XT Immunostainer (Ventana Medical Systems, Tucson, Arizona, USA) using established protocols. For dilutions and antibody details, see Online resource 1.
BRAF V600E, IDH1 R132H and H3 K27M immunohistochemistry was scored as either positive or negative in the tumour cells. Loss of nuclear ATRX expression was considered, when more than 80% of tumour cell nuclei showed loss of expression while nuclei of intermingled non-neoplastic cells serving as internal control were positive [18]. Slides were scanned either on a NanoZoomer Digital Slide Scanner (Hamamatsu, Hamamatsu, Japan) or an AT2 Aperio Digital Pathology Slide Scanner (Leica Biosystems, Wetzlar, Germany) and photographed using Aperio ImageScope software (v11.0.2.725, Aperio Technologies, Vista, California, USA).

DNA extraction and methylation data generation

DNA was extracted from FFPE or fresh frozen tissue using the automated Maxwell system (Promega, Fitchburg, Massachusetts, USA) according to the manufacturer's instructions. DNA concentration was determined using the Qubit dsDNA BR Assay kit (Invitrogen, Carlsbad, California, USA) following the producer's guidelines. From each tissue sample 200 to 500 ng of DNA were processed for DNA methylation analysis. Either the Infinium HumanMethylation450 Bead-Chip (450k) array or the Infinium MethylationEPIC array BeadChip (850K) (Illumina, Carlsbad, California, USA) were used to determine the DNA methylation status of CpG sites according to the manufacturer's instructions. From cases 6 and 43 DNA was extracted from two different areas (glial and neuronal fraction). Therefore, 56 DNA samples were gathered from 54 patients.

Methylation-based classification: unsupervised t-SNE/UMAP analyses, classifier predictions and copy number profile calculation

Initially, a t-SNE (t-distributed stochastic neighbour embedding, see abbreviations) plot was computed via the R package Rtsne (https://github.com/jkrijthe/Rtsne) using the 20,000 most variable CpG sites according to standard deviation, 3,000 iterations, a perplexity value of 10 and selected reference classes. In addition, the methylation profiles of all tumours were matched with unselected reference classes in a more comprehensive t-SNE plot comprising 90,000 tumours so far analysed via the Department of Neuropathology Heidelberg, the DKFZ and the website https://www.molecularneuropathology.org [19]. In addition, a UMAP (uniform manifold approximation and projection, see abbreviations) analysis was performed with the reference classes of the brain tumour classifier v11b4 using the 20,000 most variable CpG sites according to standard deviation and a minimum distance of 0.1.
In a second step, DNA methylation profiles were classified using the brain tumour classifier versions V11b4, V12.3 and V12.5 (https://www.molecularneuropathology.org/mnp/classifiers) [19].
In addition, copy number profiles were calculated from the methylation array data as previously described using the 'conumee' package in R (http://bioconductor.org/packages/release/bioc/html/conumee.html).

Sanger sequencing, DNA panel sequencing, and RNA sequencing

Sequencing of the hot-spot mutations in *H3-3A*, *HIST1H3B*, *BRAF*, *IDH1*, *IDH2* and the *TERT* promoter was performed according to standard protocols. Primer sequences and Refseq NM accession numbers for the respective genes are listed in Online resource 2. For the amplification reaction, the following reagents were used: 12.5 µl of Go Taq G2 DNA polymerase (Promega, Madison, Wisconsin, United States), 1.25 µl forward primer (10 pmol/µl), 1.25 µl reverse primer (10 pmol/µl), 8.0 µl nuclease free water and 2 µl template DNA (approximately 25 ng/µl). PCR conditions are listed in Online resource 3. For subsets of tumours, gene panel sequencing (n=12) or RNA sequencing (n=3) were performed as previously described [20, 21]. Gene panel sequencing data were filtered as follows: exonic and splicing single nucleotide variants were selected. Synonymous and stop loss variants were not considered. Thereafter, variants with a frequency not exceeding 0.1% in the healthy population as well as undescribed variants were selected according to the 1000 Genomes Project database. Variants described as known polymorphisms in the Single Nucleotide Polymorphism database dbSNP, version 138 (https://www.ncbi.nlm.nih.gov/projects/SNP/snp_summary.cgi?view+summary=view+summary&build_id=138) were not considered. Insertions and deletions were filtered for exonic

frameshift changes that were not yet detected in the healthy population according to the 1000 Genomes Project database and that were not present in the dbSNP database. The remaining items (nonsynonymous, stop gain or splice site variants, frameshift insertions/deletions) were evaluated for their potential clinic-pathological relevance using the databases http://cancer.sanger.ac.uk/cosmic; http://www.ncbi.nlm.nih.gov/clinvar/; https://varsome.com/. According to these databases, variants were categorized as outlined in Online resource 4. A full list of the genes represented in the applied gene panel is provided in Online resource 5. The deFuse and arriba software tools [22] were used to identify gene fusions (https://sourceforge.net/projects/defuse/; https://github.com/suhrig/arriba/).

Statistical analysis and reference dataset

The DNA methylation array data were processed with the R/Bioconductor package minfi (version 1.20) [1]. The reference classes of the t-SNE analysis were: ganglioglioma (GG; 14 cases); IDH glioma, subclass astrocytoma (A IDH; 14 cases), IDH glioma, subclass high-grade astrocytoma (A IDH HG; 15 cases); diffuse midline glioma, H3 K27 altered (DMG K27; 13 cases); glioblastoma (GBM) of the midline (GBM MID; 15 cases); GBM, *MYCN* subtype (GBM MYCN; 12 cases); GBM, mesenchymal subtype (GBM MES; 15 cases); GBM, RTK I subtype (GBM RTK I; 15 cases); GBM, RTK II subtype (GBM RTK II; 14 cases); GBM, RTK III subtype (GBM RTK III; 15 cases); pleomorphic xanthoastrocytoma (PXA; 27 cases); high-grade astrocytoma with piloid features (HGAP; 15 cases); pilocytic astrocytoma (PA) of the supratentorial hemispheres and ganglioglioma (PA CORT/GG; 14 cases); PA of the posterior fossa (PA PF; 15 cases); PA of the midline (PA MID; 13 cases); dysembryoplastic neuroepithelial tumour (DNET; 15 cases); diffuse leptomeningeal glioneuronal tumour (DLGNT; 9 cases); ependymoma, *RELA* fusion-positive (EPN RELA; 15 cases); atypical teratoid/rhabdoid tumour, subclass *MYC* (ATRT MYC; 15 cases); desmoplastic myxoid tumour, *SMARCB1*-mutant (DMT SMARCB1; 9 cases); infantile hemispheric glioma (IHG; 10 cases); subependymal giant cell astrocytoma (SEGA, 11 cases); desmoplastic infantile astrocytoma/ganglioglioma (DIG/DIA; 8 cases); supratentorial subependymoma (SEPN SUP; 10 cases); neuroepithelial tumour *PLAGL1* fusion-positive (EPN ST 1; 15 cases) and control tissue, hemispheric cortex (HEMI CORT; 10 cases). The characteristics of the reference methylation classes (MCs) are described under https://www.molecularneuropathology.org/mnp/classifiers [4].

Results

aGG was primarily diagnosed in young adults with a predilection for the temporal region

Median age of the 54 patients was 25 years ranging from 1 to 81 years. The male/female ratio of 1.2 demonstrates a slight male predominance consistent with previous reports [5, 10]. The tumour localization was known for 45 patients, with 87% in supratentorial and 18% in infratentorial compartments. Half of the tumours were located in the temporal lobe, 20% in the frontal lobe and the remaining fraction in other areas.

aGG presented with heterogeneous histological features

The aGGs in our cohort exhibited highly variable histological patterns precluding the definition of general histological criteria. Online resource 6 provides an overview of the histological features. Most aGGs showed a predominantly glial and some a mixed glioneuronal morphology. Most of the tumours exhibited increased cellularity, moderate to high nuclear pleomorphism and diffuse infiltration into the adjacent brain tissue. In only two tumours, neuronal and glial compartments appeared spatially separated. Fig 1 shows as an exemplar the histological and immunohistochemical features of one aGG (case 50 in Online resource 8) presenting with two distinct morphologies: an oligodendroglial and a mixed glioneuronal component. In Online resource 7, the results of immunohistochemical stains are summarised with most of the tumours expressing GFAP in the majority and synaptophysin in a lower fraction of the tumour cells. In approximately half of the aGGs, CD34 expression was observed [1]. The Ki67 index was highly variable with a median of 10% and a range from 1% up to 70%. Online resource 8 provides morphological and immunohistochemical findings of each tumour.

Methylation profiles of aGGs were assigned to various methylation clusters in unsupervised analyses and to various methylation classes of the brain tumour classifier

Initially, the methylation profiles of the aGGs were clustered in unsupervised analyses comprising a t-SNE plot (Fig 2) and a UMAP plot together with 342 selected reference tumours or control tissues. In addition, the methylation profiles of the aGGs were analysed together with methylation profiles of 90,000 unselected tumours and control tissues of the central and peripheral nervous system in a more comprehensive t-SNE. In these unsupervised analyses aGGs did not form a distinct cluster and were distributed among different glioma reference clusters, most commonly PXA, subclasses of GBM IDH wildtype, but also subclasses of IDH mutant astrocytoma and low-grade glial/glioneuronal tumours. A smaller subset also clustered to HGAP; however, these tumours could not be assigned to

HGAP after further molecular testing. Online resource 8 lists the assignment or closest vicinity of each of the cases in the t-SNE and UMAP plots.

Subsequently, array-based methylation data of all 56 samples from 54 patients diagnosed with aGG were subjected to analysis by the brain tumour classifier versions V11b4, V12.3 and V12.5 (https://www.molecularneuropathology.org/mnp/classifiers [19]). In the classifier versions V11b4/V12.3/V12.5, 29/32/36 samples matched with an established methylation class which is defined as reaching a calibrated score of at least 0.9. The classifier predictions for these samples are listed in Table 1 (see also Online resource 8). The remaining 27/24/20 samples received a sub-threshold prediction of less than 0.9.

In most aGGs single gene alterations were in line with the methylation-based classification

Previous series of aGGs reported alterations in *BRAF*, *CDKN2A/B*, the *TERT* promoter, *CDK4* and *H3-3A* [6, 13-17]. In our series *BRAF* mutations were found in 30% of the tumours. The main fraction of these reached the highest classifier scores for the MC PXA or the MCF (methylation class family) PA, whereas a subset was unclassifiable. Homozygous *CDKN2A/B* deletions were observed in 50% of cases, mainly in tumours with the highest classifier scores for the MC PXA and the MCF GBM IDH wildtype. *TERT* promoter mutations were detected in 20% of the tumours. These tumours were predominantly assigned to the MCF GBM IDH wildtype, whereas one tumour was classified as MCF diffuse paediatric-type high-grade glioma, H3 wildtype and IDH wildtype (case 20) and two tumours were allotted to the MC PXA (cases 1 and 7). *TERT* promoter mutations have been described in single cases of (anaplastic) PXAs [23, 24] and have been suggested to be associated with malignant transformation of these tumours [25, 26]. Focal amplifications occurred in 13% of tumours affecting the genes *EGFR*, *CCND2*, *MYCN*, *CDK4*, *MDM2*, *PDGFRA* and *MET* and were predominantly found in tumours assigned to the MCF GBM IDH wildtype, but also in one tumour classified as diffuse paediatric-type high-grade glioma, H3 wildtype and IDH wildtype [7] and in one with an elevated classifier score for the MC HGAP. Presence of the 7/10 signature (15%) was restricted to tumours assigned to the MCF GBM IDH wildtype. Three tumours with the highest classifier score for the MC DMG K27 harboured an *H3-3A* K27M mutation, with one additionally carrying a *BRAF* V600E mutation. RNA sequencing revealed a *PPP1CB/ALK* fusion in a tumour with an elevated classifier score for the MC IHG and an *EWSR1/PLAGL1* fusion in a tumour classified as MC EPN ST 1 (MC neuroepithelial tumour, *PLAGL1* fusion-positive) [27]. DNA panel sequencing indicated a *KIAA1549/BRAF* fusion in a tumour assigned to the reference cluster of DLGNTs. One case classified as MC

ATRT showed immunohistochemical loss of INI1 expression in the tumour cells (see Online resource 9) and a homozygous *SMARCB1* deletion in the copy number profile.

The most common integrated diagnoses were pleomorphic xanthoastrocytoma and glioblastoma, IDH wildtype

Histological and immunohistochemical findings, methylation profile, copy number variations and sequencing data were summarised to an integrated diagnosis (Online resource 8). Fig 3 shows how the integrated diagnoses were distributed among the 54 patients. The diagnosis (anaplastic) PXA was assigned to 30% of the tumours, whereas approximately 20% were categorized as GBM IDH wildtype. In four instances, the diagnosis A IDH was allotted. One or two tumours each were assigned to DMG K27, DLGNT, DNET, PA, IHG, supratentorial ependymoma, *ZFTA* fusion-positive [28], neuroepithelial tumour, *PLAGL1* fusion-positive [27] and ATRT.

Two tumours (cases 17 and 20) which would have been designated as GBM IDH wt according to the 4th edition of the CNS WHO classification turned out as diffuse paediatric-type high-grade glioma, H3 wildtype and IDH wildtype according to the 5th edition. The tumour of patient 17, who was 35 years old, was classified as MC high-grade glioma, paediatric-type *MYCN* in the classifier version V12.5 and had a *MYCN* amplification. Further analyses are necessary to clarify the fraction of adult patients among these tumours. Patient 20 was a 10-year-old child whose tumour was classified as MC diffuse paediatric-type high-grade glioma, RTK2 subtype in V12.5 and had a *TERT* promoter mutation which is compatible with this methylation class [7].

Fig 4 shows the HE-stained sections and copy number profiles of three tumours receiving the integrated diagnoses ATRT, GBM IDH wildtype and neuroepithelial tumour, *PLAGL1* fusion-positive (cases 45, 25 and 52).

The histological and molecular profiles of ten tumours (cases 36, 37, 43, 47-51, 53 and 54) were inconclusive. Clinical information, morphology and molecular alterations did not reveal any common features hinting to a separate tumour type. Nine tumours were designated as unclassifiable tumour (low-grade/high-grade) and one as diffuse midline glioma, NOS. The HE-stained sections of two of these tumours (cases 36 and 54) are shown in Fig 5.

Analysis of neuronal and glial components

In the cases 6 and 43, it was possible to separately analyse neuronal and glial components. The HE-stained sections and copy number profiles of these tumours are shown in Online resource 10 and additional molecular details in Online resource 8. We found that copy

number variations were predominantly observed in the glial component. Upon molecular analysis, the glial fraction of case 6 was diagnosed as PXA, whereas the neuronal fraction finally turned out as infiltration zone. In contrast, both the glial and the neuronal fraction of case 43 were considered as tumour subclones that both carried a *BRAF* V600E mutation. The glial fraction was assigned to the MC PA CORT/GG. A quite interesting finding in this fraction was a heterozygous deletion of chromosome arm 22q which is unusual for PA. The neuronal fraction was assigned to SEGAs in the t-SNE in Fig 2, but probably due to a limited set of reference classes. In the updated classifier versions V12.3 and V12.5, it was classified as MC GLIOMA NORM HI (glioma with high proportion of normal cells) and clustered accordingly in a more comprehensive t-SNE. This methylation class comprises gliomas with a high fraction of immune or stromal cells. However, the histological slides did not reveal high infiltration or normal brain tissue. Instead, enlarged and very pleomorphic tumour cells with prominent nucleoli were observed. Due to the two histologically and molecularly different compartments with unusual profiles which do not fit to a known entity, the tumour was finally considered as unclassifiable. A summary of the molecular findings and integrated diagnoses for the neuronal and glial component of cases 6 and 43 is given in Online resource 11.

Three aGGs transpired to be infiltration zone of glial tumours

After molecular analyses and histological review cases 28 and 29 were finally diagnosed as infiltration zone of GBM, whereas the neuronal component of case 6 was diagnosed as infiltration zone of PXA. The glial component of the latter presented with high cell density, heterozygous deletion of chromosome 9, homozygous deletion of *CDKN2A/B* and clustered to PXAs in the t-SNE. The histology and molecular profile were therefore indicative of PXA. In contrast, the neuronal component histologically presented with low cell density and only single, enlarged neuronal cells of unusual morphology. The methylation profile was assigned to GG; copy number alterations were not obvious (see also Online resource 11 and 8). Hence, the neuronal component was retrospectively designated as infiltration zone and the single neurons of unusual morphology were interpreted as non-neoplastic. Notably, the finding that infiltration zones reach high classifier scores for GG is not uncommon due to their oftentimes high percentage of neuronal cells. In cases 28 and 29 our initial histological impression was inconclusive. However, both molecular profiles presented with a 7/10 signature and a homozygous *CDKN2A/B* deletion and were therefore highly suggestive of glioblastoma. Re-evaluation after molecular analyses led to the consensus that the histology was at least compatible with an infiltration zone of GBM. In case 28 the low tumour cell content was also reflected by the methylation profile which was classified as MC GLIOMA

NORM HI. In contrast, case 29 was classified as MC GBM MES (see also Online resource 8).

Unclassifiable tumours had heterogeneous profiles that were not assignable to an established entity

The methylation profiles of five tumours (cases 36, 37, 48, 49, 50 in Online resource 8) were found in vicinity to the HGAP cluster in the t-SNE. However, none of them entirely fulfilled the required molecular criteria:

In case 36, a homozygous *CDKN2A/B* deletion and an *NF1* frameshift deletion were compatible with the diagnosis of HGAP. However, additional mutations in *PIK3CA* and *SETD2* were more in favour of GBM IDH wildtype. The histological (Fig 5) and molecular results suggested a high-grade glioma. However, the criteria for HGAP were not entirely fulfilled and distinction from GBM IDH wildtype was not possible.

Case 37 reached a sub-threshold score for the MC HGAP. However, the copy number profile with numerous chromosomal gains, losses and focal amplifications was unusual for this entity. Although ATRX loss and the assignment in the t-SNE were compatible with the diagnosis of HGAP, panel sequencing analysis did neither reveal a MAPK pathway alteration, nor an *ATRX* mutation. In summary, not all criteria for HGAP were met.

Case 50 clustered between HGAP, GBM MID and DLGNT upon t-SNE/UMAP analyses. Panel sequencing revealed a *KRAS* G12R hotspot mutation described in various cancers and tectal gliomas [29]. In a study on HGAPs two of 83 tumours also harboured a *KRAS* mutation, but additionally had *CDKN2A/B* and *ATRX* alterations [30]. As these were not evident in the present case, it was supposed to belong to an entity not yet characterized.

The methylation profile of case 49 was inconsistently assigned to HGAP or PXA. Besides a *CDKN2A/B* homozygous deletion, a *BRAF* D594N mutation and a *PIK3CA* E600K mutation were detected. *PIK3CA* mutations have been shown to occur in 6-15% of glioblastomas and have been linked to adverse outcome [31]. However, alterations of the PIK3 pathway were also found in other glioma entities [32, 33]. *BRAF* D594N is known as a kinase inactivating mutation leading to a reactive increase of *RAS* activity and *ERK* signalling [34]. Whether this tumour represents a rare variant of GBM, HGAP or PXA or belongs to an as yet unknown entity remained unclear.

In case 48 a *H3-3A* K27M and a *BRAF* V600E mutation were found. Single patients with glial/glioneuronal tumours and this constellation of mutations have been described. As these patients appeared to have a more favourable clinical outcome than patients with DMG K27 a

separate categorization has been suggested [35]. However, as the exact nature of these tumours is still unclear, they are not yet represented as a separate entity in the CNS WHO classification [7].

The methylation profile of case 51 was assigned to DMG K27, but no K27M mutation in *H3-3A* or *HIST1H3B* was detectable. Immunohistochemistry for loss of nuclear H3 K27me3 staining or RNA sequencing for *EZHIP* expression [36] could not be performed due to insufficient material. The tumour was therefore designated as diffuse midline glioma, NOS.

Case 43 histologically presented with a neuronal and a glial component which were spatially separated. The features of the two fractions are described above.

The histology of case 47 showed a glial/glioneuronal tumour with increased proliferation. Clinically, a second lesion was evident. Molecular analyses revealed a *BRAF* V600E mutation and whole chromosomal gains. The methylation profile was inconsistently assigned to PA CORT, DNET or GG. As the molecular findings suggested a rather low-grade glial/glioneuronal tumour, whereas the histological and clinical findings indicated a higher-grade lesion, no further grading and classification was performed.

In case 54 the histology (Fig 5) and molecular findings suggested a low-grade tumour, but were not specific for an established entity.

Histological evaluation of case 53 revealed a glial tumour with microcystic architecture and prominent calcifications, but also areas of high cell density and ependymal morphology. The methylation profile was unclassifiable, whereas several t-SNE analyses suggested some relation to ependymal tumours. DNA panel and RNA sequencing did not reveal any indicative alterations. In summary, the results in this particular case suggested a low-grade glial tumour with ependymal features.

Detailed information about clinical data, histology and molecular analyses of all tumours in this study are outlined in Online resource 8.

Discussion

The 5th edition of the WHO Classification of Tumours of the Central Nervous System states that previous studies on aGGs lacked comprehensive molecular testing and suggests further analyses to validate the existence of this entity [7]. In this study, we assessed the morphologic and molecular profiles of 54 aGGs from multiple institutions. All cases were included based on the original histological diagnosis of the submitting centre. We explored whether these tumours could be allotted to established tumour types or whether they

represent a separate entity. The majority of aGGs turned out as belonging to established glial tumour types [4], most commonly PXA and GBM IDH wildtype. Only three tumours of the aGG cohort were finally categorized as glioneuronal tumours (two as DNET and one as DLGNT).

However, many of the aGGs contained neuronal cells of partly dysplastic appearance. Although the morphology of dysmorphic ganglion cells is described in the CNS WHO classification, it is also discussed that no objective identification marker exists and that distinction from an infiltration zone of other glial tumours may be challenging [7]. Likewise, further literature in the field of glioneuronal tumours stresses diagnostic issues like the variable microscopic appearance of glial and neuronal components and the poor inter-observer agreement in the designation of gangliоglioma [1, 37]. Particularly regarding aGG, the WHO book does not indicate how many mitoses should be considered as conspicuous and how many of the described anaplastic features have to be present to justify this designation. Another complicating aspect is that ganglion cell differentiation may also be observed in other entities, for instance PXA or DLGNT [4, 7]. Hence, the constellation of features applied to assign the diagnosis of aGG may substantially depend on the observer's interpretation.. Accordingly, the results of this study indicated that a definition based on dysplastic neurons and signs of anaplasia allows for a wide spectrum of tumour types. This was supported by molecular analyses suggesting different entities. As these comprised predominantly glial tumours, our findings also raise the question, whether the dysplastic neurons observed in aGGs are more likely entrapped cells of compromised appearance due to adjacent or infiltrative tumour. The fact that three tumours of our series finally turned out as infiltration zone also underlines this issue. In summary, the wide spectrum of integrated diagnoses among aGGs indicates substantial subjectivity of this designation and in the declaration of dysplastic neurons.

Interestingly, cells with neuronal appearance have been observed in a small subset of PXAs. These tumours have been designated as composite pleomorphic xanthoastrocytoma and gangliоglioma [37-39]. The morphology of such tumours may come close to the morphology described for aGG. However, as the results of our study suggest, it has to be considered that aGG may be a misdiagnosis in case of a PXA with unusual morphology. In a recent study, we similarly found that GG, but also GBM IDH wildtype are common misdiagnoses among tumours of the MC PXA. These findings underline the importance of molecular analysis, particularly methylation-based classification, to differentiate between entities that may show histological overlap on the one hand, but also considerable histological variability on the other hand [26].

The 5th edition of the CNS WHO classification lists a new tumour type designated as diffuse high-grade glioma, paediatric-type, H3 wildtype and IDH wildtype [7]. The methylation profiles of two aGGs were allotted to the correspondent MCF in the classifier version V12.5, whereas in previous classifier versions reached elevated scores for the MCF GBM IDH wt. Indeed, their copy number profiles did not show typical features of classical adult GBM (see Online resource 8). Previous studies and empirical data also suggest that copy number aberrations of paediatric high-grade gliomas are distinct from classic GBM in adults [40-42]. Analysis of methylation profiles of diffuse high-grade gliomas, paediatric-type, H3 wildtype and IDH wildtype showed that this tumour type is a heterogeneous group comprising various MCs [42, 43]. As first results on the clinical course show that these tumours behave aggressively, CNS WHO grade 4 is considered, albeit differences in survival time between the MCs subsumed under this tumour type are observed [7, 42].

One tumour with aGG morphology (case 45, Fig 4) turned out to be ATRT. Single cases of glial/glioneuronal tumours transforming to ATRT have been described [44]. Recently, a cohort of tumours with epigenetic similarity to ATRT designated Low-grade diffusely infiltrative tumours, *SMARCB1*-mutant has been published. Two of these tumours showed high-grade areas and were initially considered as ATRT with a ganglioglioma component [45]. These data suggest that in unclear cases of aGG INI1/*SMARCB1* testing should be considered.

Case 52 was designated as neuroepithelial tumour, *PLAGL1* fusion-positive, histologically presented as clustered small, round tumour cells with intermingled ganglion cells (Fig 4) and had an *EWSR1/PLAGL1* fusion. In a case series of glial/glioneuronal tumours with unusual *EWSR1* fusions a tumour with similar histology and this particular alteration has been reported [46]. A recent study about the histological and molecular characteristics of *PLAGL1* fusion-positive neuroepithelial tumours described a heterogeneous morphology with a high fraction of cases showing ependymoma-like features [27].

Our study further showed that ten tumours with heterogeneous histological and molecular profiles could not be allotted to an established WHO diagnosis and also did not build a separate methylation cluster. For these tumours, discrepancies between the morphology, the positioning in comprehensive t-SNE analyses, the classifier predictions, and single molecular parameters were evident. Moreover, molecular alterations with unclear diagnostic significance were frequently detected, for instance combined *H3-3A* K27M and *BRAF* V600E mutation (case 48) [35, 47], a *KRAS* G12R mutation (case 50), combined *BRAF* D594N and *PIK3CA* E600K mutation (case 49), a *BRAF* V600E mutation in combination with chromosome 22q loss (case 43) and others. Taken together, the heterogeneous histology as

well as mutational and methylation profiles provided neither evidence for a known entity, nor for a group suggestive of a new tumour type beyond the 5th edition of the CNS WHO classification.

The methylation profiles of seven aGGs were assigned to the reference cluster of HGAPs (see Fig 2). Although HGAPs may comprise a wide spectrum of morphological features, a neuronal or glioneuronal appearance has not been observed [30]. Hence, it is not surprising that after histological re-evaluation and molecular testing the integrated diagnosis of HGAP was not assigned to any of these cases. After taking the molecular results into account, five of these tumours were finally designated as unclassifiable, mostly because inconclusive molecular constellations, whereas two cases were diagnosed as GBM IDH wildtype and DMG K27 (Online resource 8). Further investigations are necessary to clarify whether the five tumours with unclear molecular findings may belong to an unusual subgroup of HGAP or to other types of high-grade glioma which have not yet been described.

As a limitation of this work, we considered that single types or subtypes defined in the CNS WHO classification may possibly not be assignable or even distinguishable from other types by methylation profile. One example to mention is multinodular and vacuolating neuronal tumour. Another aspect to keep in mind is that, in single instances, the classifier is not able to distinguish neuronal and glial subtypes of related entities. This is the case in desmoplastic infantile ganglioglioma versus astrocytoma, but also in some examples of hemispheric pilocytic astrocytoma versus ganglioglioma. For these entities, common methylation classes, namely MC PA CORT/GG and MC DIG/DIA, exist despite histological differences with regard to the ratio of glial and neuronal components. The fact that a relevant fraction of aGGs molecularly turned out to be PXAs therefore raises the question whether some of these tumours may similarly represent neuronal and glial predominant variants of a molecular entity with a common methylation profile. Recent analyses of the molecular landscape of composite PXAs and GGs further underline this consideration. Notably, both components of these tumours were positive for *BRAF* V600E, whereas selectively in the PXA component a homozygous *CDKN2A/B* deletion/p16 loss and a higher number of chromosomal aberrations were obvious. Hence, these composite tumours were suggested to represent a stage of progression from GG to PXA [48, 49]. Further, more comprehensive analyses like whole genome or proteomic approaches may serve to further address this issue and to clarify whether this also applies for tumours designated as aGG.

Conclusion

Our results suggest that most tumours with the histological diagnosis of aGG belong to established CNS WHO tumour types. A small fraction was not assignable, but showed

heterogeneous histological and molecular profiles. As common features pointing to a separate tumour type or subtype were not evident in this subset of cases, these tumours may belong to various, currently uncharacterized entities. Because reliance solely on the assignment in a t-SNE plot or the classifier prediction may therefore be misleading, comprehensive molecular testing such as next generation sequencing of DNA and RNA is strongly recommended. In summary, the data of this study indicate that the histological designation of aGG may represent a wide spectrum of entities and should therefore be used with caution. Fig 6 suggests an algorithm for a reasonable and systematic molecular workup which might help with further classification of difficult cases.

Acknowledgements

We thank the Genomics and Proteomics Core Facility of the German Cancer Research Centre (DKFZ) for conducting the methylation analyses for a part of the aGG series. We thank the DKFZ Heidelberg Centre for Personalized Oncology (DKFZ-HIPO) for technical support and funding through HIPO_036. In parts, this work was supported by an Illumina Medical Research Grant and the German Cancer Consortium (DKTK) joint funding project 'Next Generation Molecular Diagnostics of Malignant Gliomas'. Annekathrin Reinhardt was funded by the Else Kröner Research College in the framework of her participation in the Research College of Neurooncology, University Hospital Heidelberg.

Author contributions:

Author	AvD	AR	KP	DC	others
Conceptualisation of the project	x	x	x	x	
Supervision of the project	x				
Data inquiry	x	x	x	x	
Data analysis	x	x	x	x	
Manuscript writing	x	x			
Contribution of tissue or patient information	x	x	x	x	x
Suggestions about manuscript design or content	x	x	x	x	x
Critical review and approval of the manuscript	x	x	x	x	x

Conflicts of interest

AvD, DC, MS and DS have pending patents on DNA methylation-based methods for classifying tumour species/tumour species of the brain. FS declares an honorary from Illumina. WW reports to be inventor and patent-holder on 'Peptides for use in treating or diagnosing IDH1R132H positive cancers' (EP2800580B1) and 'Cancer therapy with an oncolytic virus combined with a checkpoint inhibitor' (US11027013B2). He consulted for Apogenix, Astra Zeneca, Bayer, Enterome, Medac, MSD, and Roche/Genentech with

honoraria paid to the Medical Faculty at the University of Heidelberg. SP declares a grant from ITCC-P4 companies: Lilly, Roche, Pfizer, Charles River, BayerHealth Care, Pharma Mar, Amgen, Sanofi, Astra Zeneca, Servier. The other authors do not declare any competing interests.

Ethical approval

Tissue collection and processing as well as data collection were performed in compliance with local ethics regulations and approval.

References

1. Blumcke I, Wiestler OD. Gangliogliomas: an intriguing tumor entity associated with focal epilepsies. *J Neuropathol Exp Neurol* 2002;61(7):575-584.
2. Zaky W, Patil SS, Park M, Liu D, Wang WL, Wani KM, Calle S, Ketonen L, Khatua S. Ganglioglioma in children and young adults: single institution experience and review of the literature. *J Neurooncol* 2018;139(3):739-747.
3. Yust-Katz S, Anderson MD, Liu D, Wu J, Yuan Y, Olar A, Fuller GN, Brown PD, de-Groot JF. Clinical and prognostic features of adult patients with gangliogliomas. *Neuro Oncol* 2014;16(3):409-413.
4. Louis DN, Perry A, Reifenberger G, von Deimling A, Figarella-Branger D, Cavenee WK, Ohgaki H, Wiestler OD, Kleihues P, Ellison DW. The 2016 World Health Organization Classification of Tumors of the Central Nervous System: a summary. *Acta Neuropathol* 2016;131(6):803-820.
5. Lucas JT, Jr., Huang AJ, Mott RT, Lesser GJ, Tatter SB, Chan MD. Anaplastic ganglioglioma: a report of three cases and review of the literature. *J Neurooncol* 2015;123(1):171-177.
6. Zanello M, Pages M, Tauziede-Espariat A, Saffroy R, Puget S, Lacroix L, Dezamis E, Devaux B, Chretien F, Andreiuolo F *et al*. Clinical, Imaging, Histopathological and Molecular Characterization of Anaplastic Ganglioglioma. *J Neuropathol Exp Neurol* 2016;75(10):971-980.
7. WHO Classification of Tumours Editorial Board. Central nervous system tumours. Lyon (France): International Agency for Research on Cancer; 2021. (WHO classification of tumours series, 5th ed.; vol. 6). https://publications.iarc.fr/601.
8. Mallick S, Benson R, Melgandi W, Giridhar P, Rath GK. Impact of surgery, adjuvant treatment, and other prognostic factors in the management of anaplastic ganglioglioma. *Childs Nerv Syst* 2018;34(6):1207-1213.
9. Bouali S, Ben Said I, Zehani A, Drissi C, Bouhoula A, Kallel J, Jemel H. Pediatric Intracranial Anaplastic Gangliogliomas: Illustrative Case and Systematic Review. *World Neurosurg* 2018;119:220-231.
10. Selvanathan SK, Hammouche S, Salminen HJ, Jenkinson MD. Outcome and prognostic features in anaplastic ganglioglioma: analysis of cases from the SEER database. *J Neurooncol* 2011;105(3):539-545.
11. Terrier LM, Bauchet L, Rigau V, Amelot A, Zouaoui S, Filipiak I, Caille A, Almairac F, Aubriot-Lorton MH, Bergemer-Fouquet AM *et al*. Natural course and prognosis of anaplastic gangliogliomas: a multicenter retrospective study of 43 cases from the French Brain Tumor Database. *Neuro Oncol* 2017;19(5):678-688.
12. Luyken C, Blumcke I, Fimmers R, Urbach H, Wiestler OD, Schramm J. Supratentorial gangliogliomas: histopathologic grading and tumor recurrence in 184 patients with a median follow-up of 8 years. *Cancer* 2004;101(1):146-155.
13. von Deimling A, Fimmers R, Schmidt MC, Bender B, Fassbender F, Nagel J, Jahnke R, Kaskel P, Duerr EM, Koopmann J *et al*. Comprehensive allelotype and genetic anaysis of 466 human nervous system tumors. *J Neuropathol Exp Neurol* 2000;59(6):544-558.
14. Pandita A, Balasubramaniam A, Perrin R, Shannon P, Guha A. Malignant and benign ganglioglioma: a pathological and molecular study. *Neuro Oncol* 2007;9(2):124-134.
15. Joyon N, Tauziede-Espariat A, Alentorn A, Giry M, Castel D, Capelle L, Zanello M, Varlet P, Bielle F. K27M mutation in H3F3A in ganglioglioma grade I with spontaneous malignant transformation extends the histopathological spectrum of the histone H3 oncogenic pathway. *Neuropathol Appl Neurobiol* 2017;43(3):271-276.
16. Hoischen A, Ehrler M, Fassunke J, Simon M, Baudis M, Landwehr C, Radlwimmer B, Lichter P, Schramm J, Becker AJ *et al*. Comprehensive characterization of genomic aberrations in gangliogliomas by CGH, array-based CGH and interphase FISH. *Brain Pathol* 2008;18(3):326-337.

17. Mizuguchi M, Takashima S, Yamanouchi H, Nakazato Y, Mitani H, Hino O. Novel cerebral lesions in the Eker rat model of tuberous sclerosis: cortical tuber and anaplastic ganglioglioma. *J Neuropathol Exp Neurol* 2000;59(3):188-196.
18. Reuss DE, Sahm F, Schrimpf D, Wiestler B, Capper D, Koelsche C, Schweizer L, Korshunov A, Jones DT, Hovestadt V *et al*. ATRX and IDH1-R132H immunohistochemistry with subsequent copy number analysis and IDH sequencing as a basis for an "integrated" diagnostic approach for adult astrocytoma, oligodendroglioma and glioblastoma. *Acta Neuropathol* 2015;129(1):133-146.
19. Capper D, Jones DTW, Sill M, Hovestadt V, Schrimpf D, Sturm D, Koelsche C, Sahm F, Chavez L, Reuss DE *et al*. DNA methylation-based classification of central nervous system tumours. *Nature* 2018;555(7697):469-474.
20. Stichel D, Schrimpf D, Casalini B, Meyer J, Wefers AK, Sievers P, Korshunov A, Koelsche C, Reuss DE, Reinhardt A *et al*. Routine RNA sequencing of formalin-fixed paraffin-embedded specimens in neuropathology diagnostics identifies diagnostically and therapeutically relevant gene fusions. *Acta Neuropathol* 2019;138(5):827-835.
21. Sahm F, Schrimpf D, Jones DT, Meyer J, Kratz A, Reuss D, Capper D, Koelsche C, Korshunov A, Wiestler B *et al*. Next-generation sequencing in routine brain tumor diagnostics enables an integrated diagnosis and identifies actionable targets. *Acta Neuropathol* 2016;131(6):903-910.
22. McPherson A, Hormozdiari F, Zayed A, Giuliany R, Ha G, Sun MG, Griffith M, Heravi Moussavi A, Senz J, Melnyk N *et al*. deFuse: an algorithm for gene fusion discovery in tumor RNA-Seq data. *PLoS Comput Biol* 2011;7(5):e1001138.
23. Ma C, Feng R, Chen H, Hameed NUF, Aibaidula A, Song Y, Wu J. BRAF V600E, TERT, and IDH2 Mutations in Pleomorphic Xanthoastrocytoma: Observations from a Large Case-Series Study. *World Neurosurg* 2018;120:e1225-e1233.
24. Phillips JJ, Gong H, Chen K, Joseph NM, van Ziffle J, Bastian BC, Grenert JP, Kline CN, Mueller S, Banerjee A *et al*. The genetic landscape of anaplastic pleomorphic xanthoastrocytoma. *Brain Pathol* 2019;29(1):85-96.
25. Hosono J, Nitta M, Masui K, Maruyama T, Komori T, Yokoo H, Saito T, Muragaki Y, Kawamata T. Role of a Promoter Mutation in TERT in Malignant Transformation of Pleomorphic Xanthoastrocytoma. *World Neurosurg* 2019;126:624-630.
26. Ebrahimi A, Korshunov A, Reifenberger G, Capper D, Felsberg J, Trisolini E, Pollo B, Prinz M, Staszewski O, Schweizer L *et al*. Pleomorphic xanthoastrocytoma is a heterogeneous entity with pTERT mutations prognosticating shorter survival. *Acta Neuropathologica Communications* 2022;10.
27. Sievers P, Henneken SC, Blume C, Sill M, Schrimpf D, Stichel D, Okonechnikov K, Reuss DE, Benzel J, Maass KK *et al*. Recurrent fusions in PLAGL1 define a distinct subset of pediatric-type supratentorial neuroepithelial tumors. *Acta Neuropathol* 2021.
28. Ellison DW, Aldape KD, Capper D, Fouladi M, Gilbert MR, Gilbertson RJ, Hawkins C, Merchant TE, Pajtler K, Venneti S *et al*. cIMPACT-NOW update 7: advancing the molecular classification of ependymal tumors. *Brain Pathol* 2020;30(5):863-866.
29. Chiang J, Li X, Liu APY, Qaddoumi I, Acharya S, Ellison DW. Tectal glioma harbors high rates of KRAS G12R and concomitant KRAS and BRAF alterations. *Acta Neuropathol* 2020;139(3):601-602.
30. Reinhardt A, Stichel D, Schrimpf D, Sahm F, Korshunov A, Reuss DE, Koelsche C, Huang K, Wefers AK, Hovestadt V *et al*. Anaplastic astrocytoma with piloid features, a novel molecular class of IDH wildtype glioma with recurrent MAPK pathway, CDKN2A/B and ATRX alterations. *Acta Neuropathol* 2018;136(2):273-291.
31. Tanaka S, Batchelor TT, Iafrate AJ, Dias-Santagata D, Borger DR, Ellisen LW, Yang D, Louis DN, Cahill DP, Chi AS. PIK3CA activating mutations are associated with more disseminated disease at presentation and earlier recurrence in glioblastoma. *Acta Neuropathol Commun* 2019;7(1):66.
32. Broderick DK, Di C, Parrett TJ, Samuels YR, Cummins JM, McLendon RE, Fults DW, Velculescu VE, Bigner DD, Yan H. Mutations of PIK3CA in anaplastic

oligodendrogliomas, high-grade astrocytomas, and medulloblastomas. *Cancer Res* 2004;64(15):5048-5050.
33. Sievers P, Appay R, Schrimpf D, Stichel D, Reuss DE, Wefers AK, Reinhardt A, Coras R, Ruf VC, Schmid S *et al*. Rosette-forming glioneuronal tumors share a distinct DNA methylation profile and mutations in FGFR1, with recurrent co-mutation of PIK3CA and NF1. *Acta Neuropathol* 2019;138(3):497-504.
34. Yao Z, Yaeger R, Rodrik-Outmezguine VS, Tao A, Torres NM, Chang MT, Drosten M, Zhao H, Cecchi F, Hembrough T *et al*. Tumours with class 3 BRAF mutants are sensitive to the inhibition of activated RAS. *Nature* 2017;548(7666):234-238.
35. Pages M, Beccaria K, Boddaert N, Saffroy R, Besnard A, Castel D, Fina F, Barets D, Barret E, Lacroix L *et al*. Co-occurrence of histone H3 K27M and BRAF V600E mutations in paediatric midline grade I ganglioglioma. *Brain Pathol* 2018;28(1):103-111.
36. Castel D, Kergrohen T, Tauziede-Espariat A, Mackay A, Ghermaoui S, Lechapt E, Pfister SM, Kramm CM, Boddaert N, Blauwblomme T *et al*. Histone H3 wild-type DIPG/DMG overexpressing EZHIP extend the spectrum diffuse midline gliomas with PRC2 inhibition beyond H3-K27M mutation. *Acta Neuropathol* 2020;139(6):1109-1113.
37. Blumcke I, Coras R, Wefers AK, Capper D, Aronica E, Becker A, Honavar M, Stone TJ, Jacques TS, Miyata H *et al*. Review: Challenges in the histopathological classification of ganglioglioma and DNT: microscopic agreement studies and a preliminary genotype-phenotype analysis. *Neuropathol Appl Neurobiol* 2019;45(2):95-107.
38. Kordek R, Biernat W, Sapieja W, Alwasiak J, Liberski PP. Pleomorphic xanthoastrocytoma with a gangliomatous component: an immunohistochemical and ultrastructural study. *Acta Neuropathol* 1995;89(2):194-197.
39. Perry A, Giannini C, Scheithauer BW, Rojiani AM, Yachnis AT, Seo IS, Johnson PC, Kho J, Shapiro S. Composite pleomorphic xanthoastrocytoma and ganglioglioma: report of four cases and review of the literature. *Am J Surg Pathol* 1997;21(7):763-771.
40. Giunti L, Pantaleo M, Sardi I, Provenzano A, Magi A, Cardellicchio S, Castiglione F, Tattini L, Novara F, Buccoliero AM *et al*. Genome-wide copy number analysis in pediatric glioblastoma multiforme. *Am J Cancer Res* 2014;4(3):293-303.
41. Bax DA, Mackay A, Little SE, Carvalho D, Viana-Pereira M, Tamber N, Grigoriadis AE, Ashworth A, Reis RM, Ellison DW *et al*. A distinct spectrum of copy number aberrations in pediatric high-grade gliomas. *Clin Cancer Res* 2010;16(13):3368-3377.
42. Korshunov A, Schrimpf D, Ryzhova M, Sturm D, Chavez L, Hovestadt V, Sharma T, Habel A, Burford A, Jones C *et al*. H3-/IDH-wild type pediatric glioblastoma is comprised of molecularly and prognostically distinct subtypes with associated oncogenic drivers. *Acta Neuropathol* 2017;134(3):507-516.
43. Pfister SM, Reyes-Mugica M, Chan JKC, Hasle H, Lazar AJ, Rossi S, Ferrari A, Jarzembowski JA, Pritchard-Jones K, Hill DA *et al*. A Summary of the Inaugural WHO Classification of Pediatric Tumors: Transitioning from the Optical into the Molecular Era. *Cancer Discov* 2022;12(2):331-355.
44. Schweizer Y, Meszaros Z, Jones DTW, Koelsche C, Boudalil M, Fiesel P, Schrimpf D, Piro RM, Brehmer S, von Deimling A *et al*. Molecular Transition of an Adult Low-Grade Brain Tumor to an Atypical Teratoid/Rhabdoid Tumor Over a Time-Course of 14 Years. *J Neuropathol Exp Neurol* 2017;76(8):655-664.
45. Hasselblatt M, Thomas C, Federico A, Bens S, Hellstrom M, Casar-Borota O, Kordes U, Neumann JE, Dottermusch M, Rodriguez FJ *et al*. Low-grade diffusely infiltrative tumour (LGDIT), SMARCB1-mutant: A clinical and histopathological distinct entity showing epigenetic similarity with ATRT-MYC. *Neuropathol Appl Neurobiol* 2022.
46. Lopez-Nunez O, Cafferata B, Santi M, Ranganathan S, Pearce TM, Kulich SM, Bailey KM, Broniscer A, Rossi S, Zin A *et al*. The spectrum of rare central nervous

system (CNS) tumors with EWSR1-non-ETS fusions: experience from three pediatric institutions with review of the literature. *Brain Pathol* 2021;31(1):70-83.
47. Nguyen AT, Colin C, Nanni-Metellus I, Padovani L, Maurage CA, Varlet P, Miquel C, Uro-Coste E, Godfraind C, Lechapt-Zalcman E *et al*. Evidence for BRAF V600E and H3F3A K27M double mutations in paediatric glial and glioneuronal tumours. *Neuropathol Appl Neurobiol* 2015;41(3):403-408.
48. Wang Y, Wang L, Blumcke I, Zhang W, Fu Y, Shan Y, Piao Y, Zhao G. Integrated genotype-phenotype analysis of long-term epilepsy-associated ganglioglioma. *Brain Pathol* 2022;32(1):e13011.
49. Lucas CG, Davidson CJ, Alashari M, Putnam AR, Whipple NS, Bruggers CS, Mendez JS, Cheshier SH, Walker JB, Ramani B *et al*. Targeted Next-Generation Sequencing Reveals Divergent Clonal Evolution in Components of Composite Pleomorphic Xanthoastrocytoma-Ganglioglioma. *J Neuropathol Exp Neurol* 2022.

Fig 1

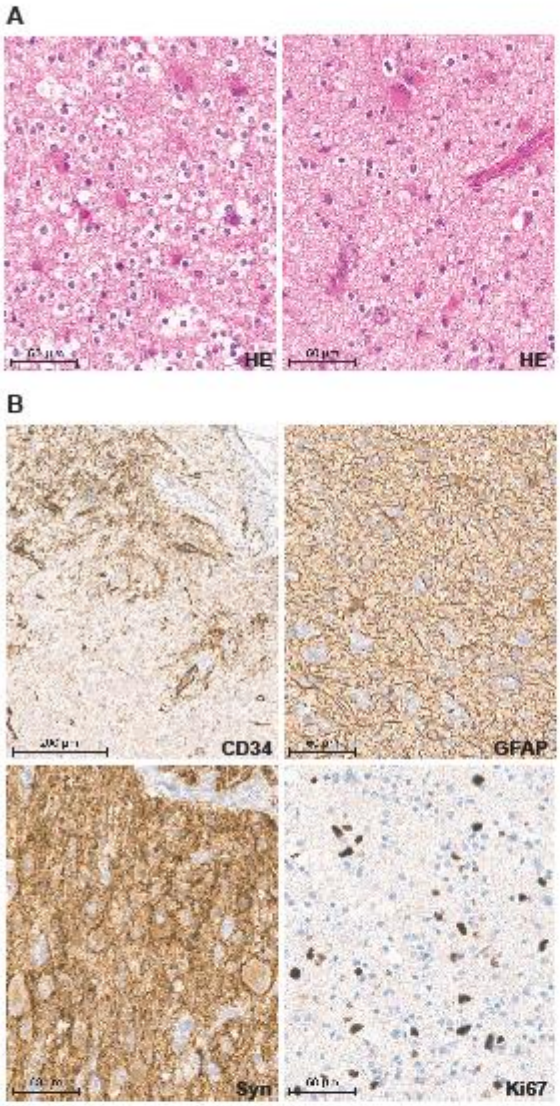

Figure 1

Histological and immunohistochemical features of a tumour originally diagnosed as aGG and presenting with two distinct morphologies (case 50 in Online resource 8). a) HE-stained sections of an area of oligodendroglial (left) and another area of glioneuronal (right) morphology. b) The CD34 stains (upper left) showed focally positive tumour cell clusters, GFAP and synaptophysin (upper right and lower left) were both widely expressed with negative staining of ganglion cells for GFAP and positive staining of ganglion cells for synaptophysin; the Ki67 proliferation index was moderately elevated (lower right).

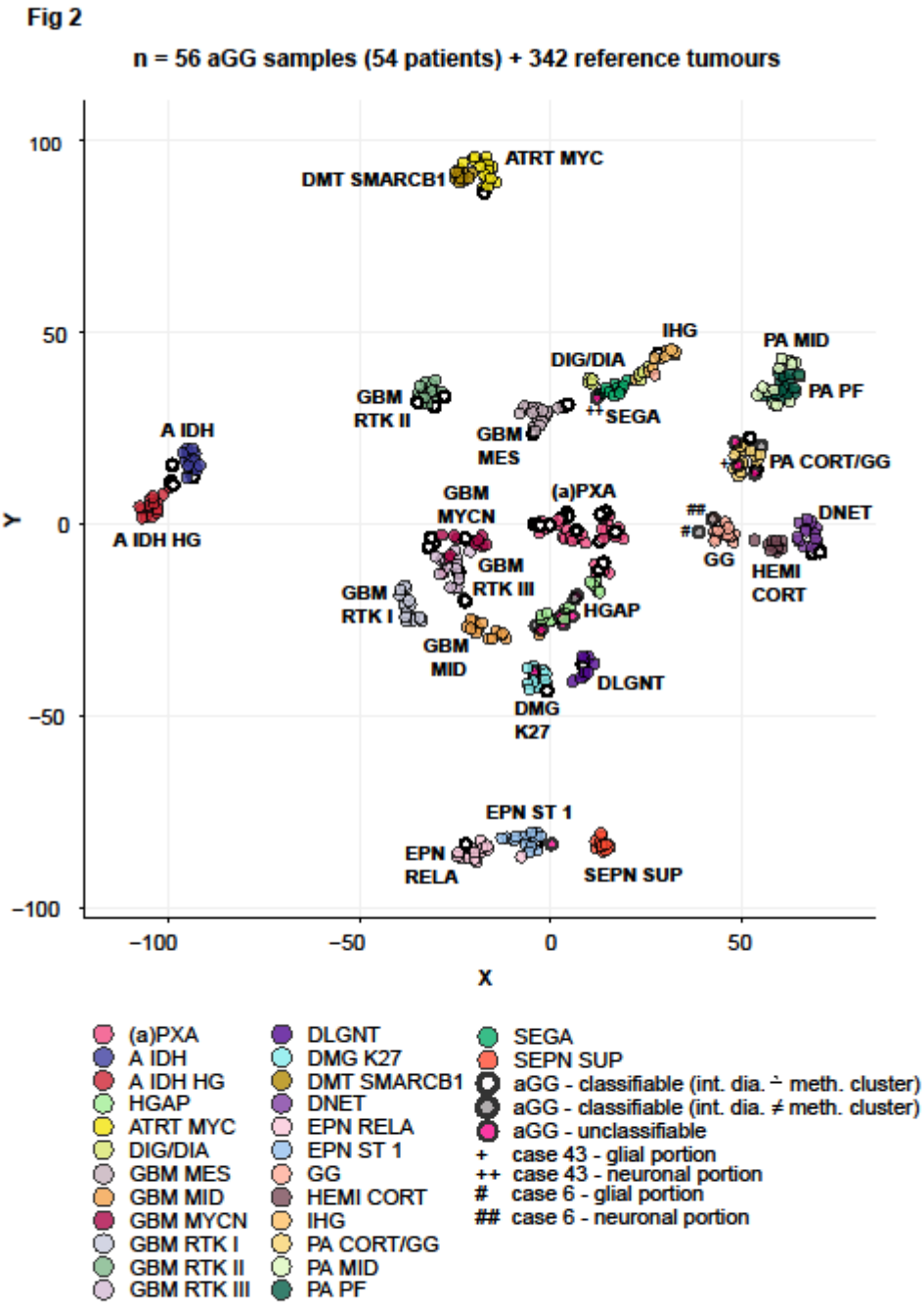

Figure 2

t-SNE analysis of 54 tumours* with the histological diagnosis of anaplastic ganglioglioma, indicated in black circles, and 342 reference cases of established glioma methylation classes, indicated in different colours. Tumours of the same class are depicted in one colour.

For this analysis the 20,000 most variably methylated CpG islands were used. Reference methylation classes: A IDH - IDH glioma, subclass astrocytoma; A IDH HG - IDH glioma, subclass high-grade astrocytoma; HGAP - high-grade astrocytoma with piloid features, DMG K27 - diffuse midline glioma, H3 K27 altered; GBM MID - glioblastoma, IDH wildtype, subclass midline; GBM MES - glioblastoma, IDH wildtype, subclass mesenchymal; GBM RTK I - glioblastoma, IDH wildtype, subclass RTK I; GBM RTK II - glioblastoma, IDH wildtype, subclass RTK II; GBM RTK III - glioblastoma, IDH wildtype, subclass RTK III; GBM MYCN - glioblastoma, IDH wildtype, subclass MYCN; PXA - (anaplastic) pleomorphic xanthoastrocytoma; DLGNT - diffuse leptomeningeal glioneuronal tumour; ATRT MYC – atypical teratoid/rhabdoid tumour, subclass MYC; PA CORT/GG – low-grade glioma, subclass hemispheric pilocytic astrocytoma and ganglioglioma; PA MID – low-grade glioma, subclass midline pilocytic astrocytoma; PA PF – low-grade glioma, subclass posterior fossa pilocytic astrocytoma; DNET – low-grade glioma, dysembryoplastic neuroepithelial tumour; GG – low-grade glioma, ganglioglioma; IHG - infantile hemispheric glioma; SEGA – low-grade glioma, subependymal giant cell astrocytoma; DIG/DIA – low-grade glioma, desmoplastic infantile astrocytoma/ganglioglioma; SEPN SUP - subependymoma, supratentorial; EPN RELA - ependymoma, *RELA* fusion-positive; EPN ST 1 - neuroepithelial tumour, *PLAGL1* fusion-positive; DMT SMARCB1 - desmoplastic myxoid tumour, SMARCB1-mutant; HEMI CORT - control tissue, hemispheric cortex; int. dia. - integrated diagnosis; meth. cluster - methylation cluster. *Two patients are represented twice: # case 6 - glial portion, ## case 6 - neuronal portion; + case 43 - glial portion; ++ case 43 - neuronal portion.

Fig 3

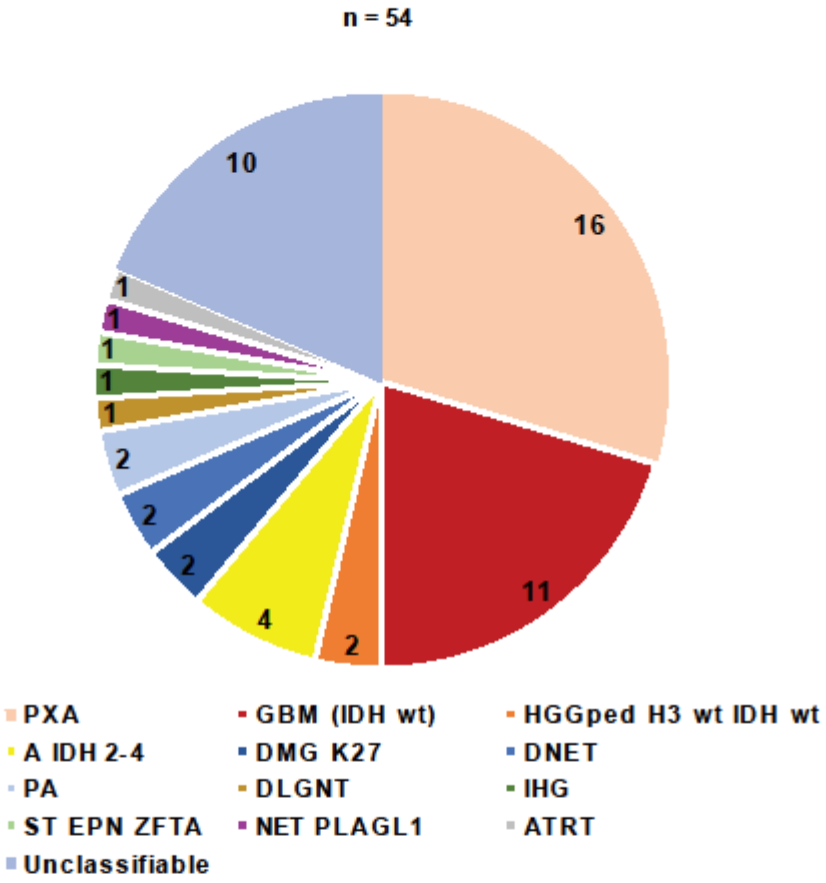

Figure 3

Distribution of integrated diagnoses among the tumours of 54 patients histologically diagnosed as anaplastic ganglioglioma. PXA - pleomorphic xanthoastrocytoma, CNS WHO

grades 2-3; GBM (IDH wt) - glioblastoma IDH wildtype, CNS WHO grade 4; HGGped H3 wt IDH wt - diffuse paediatric-type high-grade glioma, H3 wildtype, IDH wildtype (CNS WHO grade 4); A IDH 2-4 - astrocytoma IDH mutant, CNS WHO grades 2-4; DMG K27 - diffuse midline glioma H3 K27 altered, CNS WHO grade 4; DNET - dysembryoplastic neuroepithelial tumour, CNS WHO grade 1; PA - pilocytic astrocytoma, CNS WHO grade 1; DLGNT - diffuse leptomeningeal glioneuronal tumour; IHG - infant-type hemispheric glioma; ST EPN ZFTA - supratentorial ependymoma *ZFTA* fusion-positive; NET PLAGL1 - neuroepithelial tumour *PLAGL1* fusion-positive; ATRT - atypical teratoid/rhabdoid tumour, CNS WHO grade 4.

Fig 4

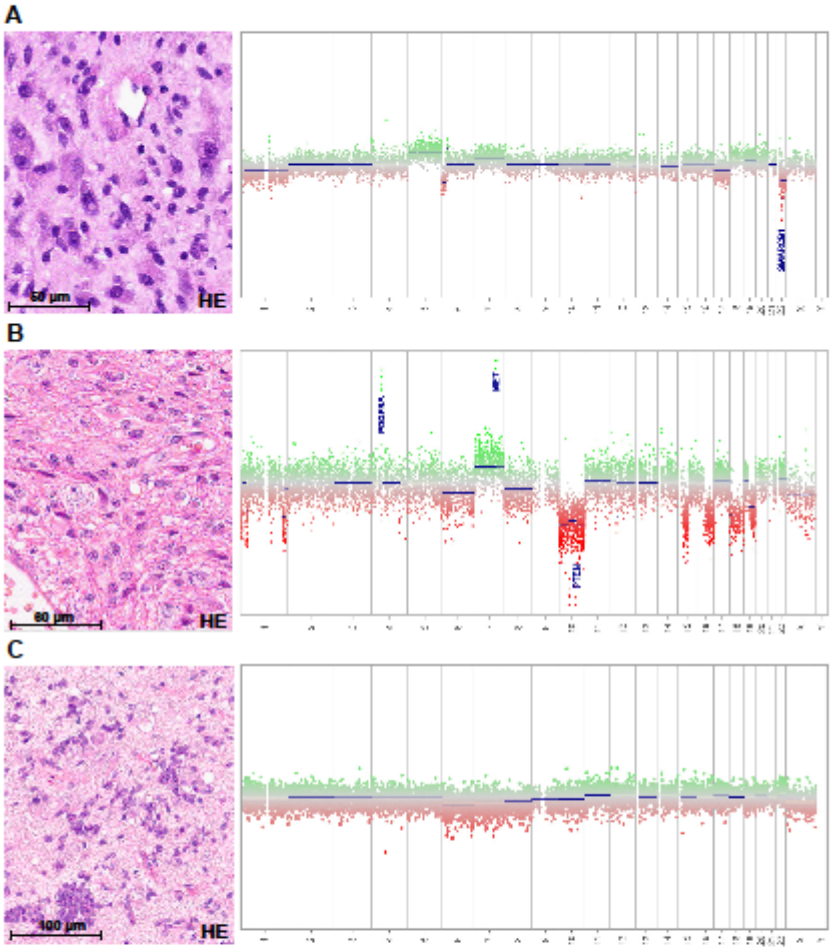

Figure 4

HE-stained sections and summary copy number profiles of three tumours with the histological diagnosis of anaplastic ganglioglioma and revised integrated diagnosis after

molecular analyses. a) Atypical teratoid/rhabdoid tumour, CNS WHO grade 4 (case 45): the HE-stained section shows cells with neuronal appearance and prominent nucleoli; some of them are binucleated; moreover, smaller cells with partially elongated nuclei are observed; in the copy number profile a loss of chromosome arm 22q including a focal homozygous deletion of *SMARCB1* is evident. Interestingly, INI1 loss was observed in the smaller cell component only (see also Online resource 9). b) Glioblastoma, IDH wildtype, CNS WHO grade 4 (case 25): the HE-stained section reveals a pleomorphic glial tumour with single enlarged cells with prominent nucleoli; in the copy number profile a 7/10 signature, amplifications of *PDGFRA* and *MET* and a homozygous *PTEN* deletion are evident. c) Neuroepithelial tumour, *EWSR1/PLAGL1* fusion-positive (case 52): histology shows a small round cell tumour with intermingled ganglion cells; the copy number profile does not show indications of copy number gains or losses.

Fig 5

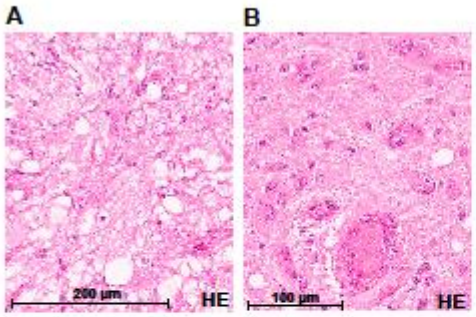

Figure 5

HE-stained sections of two tumours with the histological diagnosis of anaplastic ganglioglioma and unclear integrated diagnosis, even after molecular analyses. a)

Unclassifiable tumour (low-grade) (case 54): pleomorphic neuroectodermal tumour with microcystic architecture, vesicular appearing nuclei and prominent nucleoli; the copy number profile (not shown) revealed no indications for chromosomal aberrations. b) Unclassifiable tumour (high-grade) (case 36): in the HE-stained section multi-layered vessels and pleomorphic tumour cells are visible, among these a binucleated tumour cell with prominent nucleoli; the copy number profile (not shown) revealed a homozygous *CDKN2A/B* deletion.

Fig 6

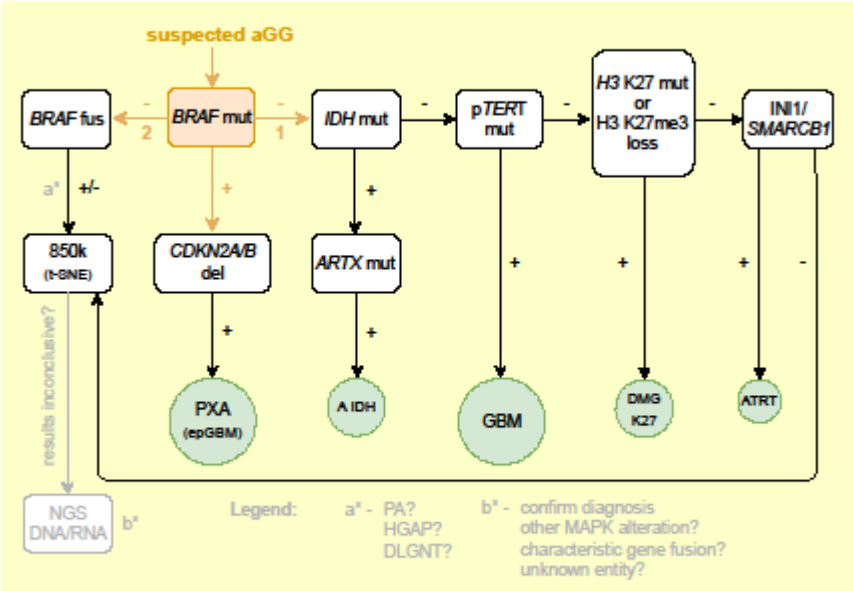

Figure 6

Proposal of an algorithm for the differential diagnostic workup of anaplastic ganglioglioma. Abbreviations: + positive/alteration present, - negative/alteration absent, fus - fusion, mut - mutation, del - deletion, p - promoter, H3 K27 – lysine 27 of a Histone H3 family protein, H3 K27me3 - immunohistochemical stain indicating tri-methylation of lysine 27 in a Histone H3 family protein, 850k - DNA methylation analysis, t-SNE - t-distributed stochastic neighbour embedding, NGS - next generation sequencing, aGG - anaplastic ganglioglioma, PA - pilocytic astrocytoma, HGAP - high-grade astrocytoma with piloid features, DLGNT - diffuse leptomeningeal glioneuronal tumour, MAPK - mitogen activated kinase, PXA - pleomorphic xanthoastrocytoma, epGMB - epithelioid glioblastoma, GBM - glioblastoma (IDH wildtype), A IDH - astrocytoma IDH mutant, DMG K27 - diffuse midline glioma H3 K27 altered, ATRT - atypical teratoid/rhabdoid tumour.

Graphical abstract

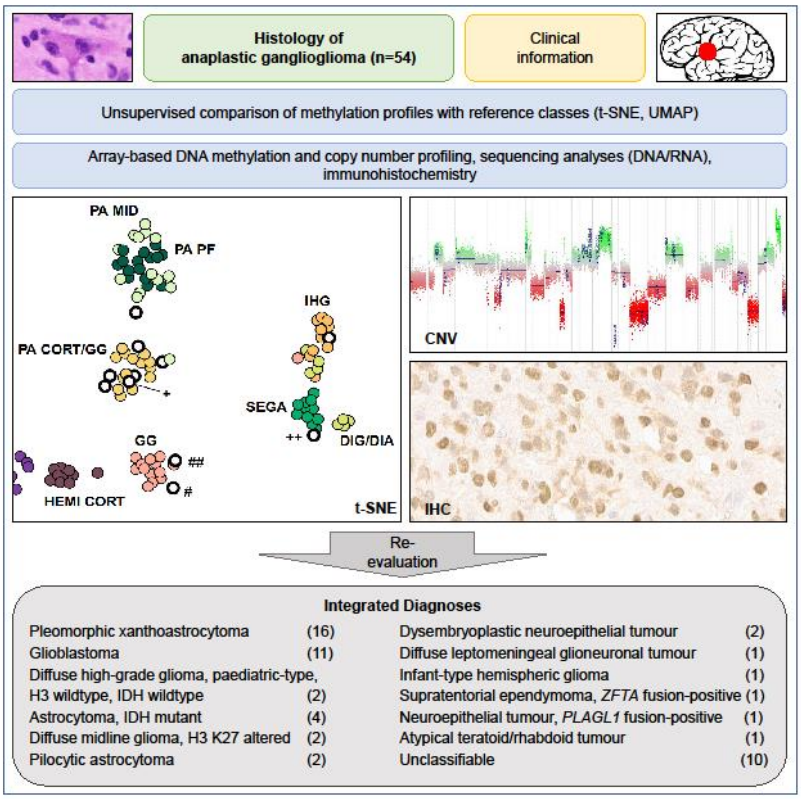

Table 1

Classifier predictions of the samples with scores of at least 0.9 in the brain tumour classifier versions V11b4, V12.3 and V12.5: MC - methylation class, MCF - methylation class family, PXA - pleomorphic xanthoastrocytoma, GBM - glioblastoma, PA - pilocytic astrocytoma, GG - ganglioglioma, DNET - dysembryoplastic neuroepithelial tumour, DLGNT - diffuse leptomeningeal glioneuronal tumour, DMG K27 - diffuse midline glioma H3 K27 altered, CTRL RB - control tissue reactive brain, GLIOMA NORM HI - glioma with high proportion of normal (immune or stromal) cells, EPN *RELA/RELA* like/*ZFTA* - ependymoma *RELA/ZFTA* fusion-positive, EPN ST 1 - supratentorial ependymoma subclass 1 (= neuroepithelial tumour, *PLAGL1* fusion-positive), ATRT - atypical teratoid/rhabdoid tumour, HGG H3 wt IDH wt - Diffuse paediatric-type high-grade glioma, H3 wildtype and IDH wildtype, LGGNT – Low-grade ganglioglial/neuroepithelial tumour.

MC/MCF	**V11b4**	**V12.3**	**V12.5**
MC (a)PXA	12	12	12
MCF GBM IDH wt	5	5	6
MCF HGG H3 wt IDH wt	n.a.	n.a.	2
MCF PA/MCF LGGNT	2	2	3
MC GG	1	1	1
MC DNET	0	1	1
MC DLGNT/DLGNT 2	0	1	1
MC DMG K27	3	2	2
MCF IDH glioma	3	3	3
MC CTRL RB/GLIOMA NORM HI	2	3	3
MC EPN RELA/RELA like/ZFTA	0	1	1
MC EPN ST 1	n.a.	1	1
MCF ATRT	1	0	0
all	29	32	36